

SHEHU, H., ORAKWE, I. and GOBINA, E. 2021. Thermo-neutral methane reforming using a flow-through porous Rh-impregnated membrane catalyst reactor for carbon capture and utilisation. Presented at *8th International conference and exhibition on advanced and nanomaterials 2021 (ICANM 2021)*, 9-11 August 2021, [virtual conference]

# Thermo-neutral methane reforming using a flow-through porous Rh-impregnated membrane catalyst reactor for carbon capture and utilisation.

SHEHU, H., ORAKWE, I. and GOBINA, E.

2021

# THERMO-NEUTRAL METHANE REFORMING USING A FLOW-THROUGH POROUS RH-IMPREGNATED MEMBRANE CATALYST REACTOR FOR CARBON CAPTURE AND UTILISATION

*Habiba Shehu, Ifeyinwa Orakwe, Edward Gobina \**

Robert Gordon University, Centre for Process Integration & Membrane Technology), School of Engineering, Garthdee Road, Aberdeen AB10 7GJ

\*Corresponding author e-mail: e.gobina@rgu.ac.uk

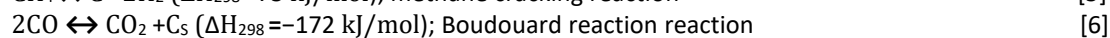
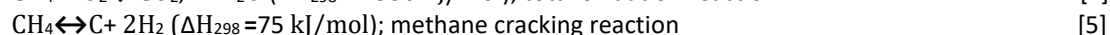
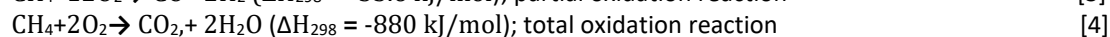
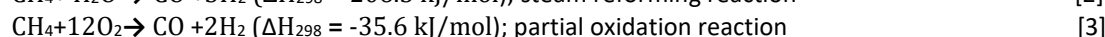
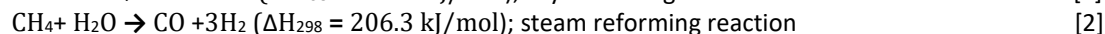
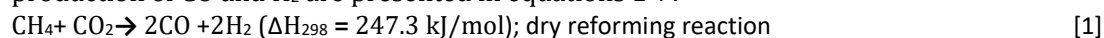
## ABSTRACT

A thermo-neutral process has been developed and tested for the carbon dioxide (CO<sub>2</sub>) reforming of methane (CH<sub>4</sub>) with oxygen (O<sub>2</sub>) and steam (H<sub>2</sub>O). A catalytic membrane reactor in which the catalytic material is dispersed within the straight through porous network was used to study this process. This design suggests an elegant route for the utilisation of waste gas streams such as vent gas and flue gas streams. It can also be used in the monetisation of stranded gas assets containing large volumes of CO<sub>2</sub>. Results have demonstrated complete conversion of all the feedstocks into synthesis gas (CO, H<sub>2</sub>) with a composition of H<sub>2</sub>/CO = 2. Synthesis gas with this composition or ranging from 1 to 2 has been identified as a key to the production of major heavy chemicals using the Fischer-Tropsch synthetic route

**Keywords:** Carbon dioxide, Reforming, Methane, Oxygen, Membrane

## INTRODUCTION

Flare and vent gases are produced in petroleum plants such as oil & gas refineries, oil & gas production and processing facilities etc. These vent and flare infrastructures have the main purpose of safely disposing off the excess hydrocarbons coming out from the facility for various reasons including opening of pressure relief valves, planned maintenance shutdown etc. The hydrocarbons present in the flare or vent stack can be used as a feedstock together with unavoidably produced CO<sub>2</sub> and processed in many ways. One of these ways is the reforming of the hydrocarbons by the CO<sub>2</sub> [1]. In a lot of instances these vent and flare streams also contain O<sub>2</sub> and water vapour (H<sub>2</sub>O) which creates the perfect feedstock for the thermo-neutral process. Other ways of handling these streams aside from venting and flaring involves separation methods in which produced CO<sub>2</sub> can be captured by methods such as adsorption, absorption or membrane separation and permanently stored in underground depleted oil & gas reservoirs. Today, adsorption of CO<sub>2</sub> is mostly used and involves amine scrubbing of the CO<sub>2</sub>. Although storage in depleted reservoirs holds promise for large-scale storage CO<sub>2</sub> sequestration, using other methods is important when viewed from safety considerations because of fears of leakages through tank or rock cracks and fissures which can occur as a result of seismic geological events. When the flue or vent gas also contains oxygen and water we may think of CO<sub>2</sub> utilisation instead of sequestration in geological reservoirs and one way of doing this is a thermo-neutral reformation process in which the CO<sub>2</sub>, CH<sub>4</sub>, O<sub>2</sub>, and H<sub>2</sub>O react to generate a mixture of CO and H<sub>2</sub>. The chemical reactions leading up to the production of CO and H<sub>2</sub> are presented in equations 1-7:



In equations 1-4, we have combined the exothermic reactions and the endothermic reactions to create a thermo-neutral process with the result that low temperature operations are possible while also achieving high conversion. While the process is elegant in this respect the dry reforming process has a major drawback which is that catalysts used in the process deactivate very rapidly caused by carbon deposition on active sites as a result of coke formation and the Boudouard reaction represented by equations 5 and 6 respectively. This is a major issue preventing commercialisation of the dry reforming process [2].

## MATERIALS AND METHODS

The schematic diagrams of the membrane operating in forced-flow mode and feed flow into the reactor used for permeation as well as reaction experiments are presented in Figures 1 and 2 respectively (CV = Control valve, MFC = Mass Flow Controller, TC = Thermocouple, GLS = Gas-Liquid separator, CD = Condenser, GC = Gas chromatograph).

Single and mixed gas permeation tests were conducted prior to the reaction tests including reduction of the catalysts in flowing hydrogen at 350<sup>o</sup> C for 10 minutes to activate the rhodium layer.

The reactor consists of a high temperature ceramic catalytic tube enclosed in a furnace with zoned heating and a power controller to control the temperature of the membrane centralized inside a stainless steel tube as shown in Figure 3. The two ends of the stainless steel shell are fitted with screw caps which through tightening create the seal by compression of moulded graphite seal rings (GEE Graphite, Dewsbury, UK) located at the top and bottom of the membrane tube. Five Ni-Cr thermocouples (Cole – Palmer, London, UK) are inserted in to the furnace (Figure 3) at the top middle and bottom through 0.32 cm bored-through fittings. The furnace used in the reactor set-up is custom designed and has four split zones (Horst, Frankfort, Germany). The first zone serves to preheat the incoming feed gases, second and third zones serve to maintain the isothermal conditions for the membrane, and fourth zone maintains the reactor temperature in order to avoid any condensation of water vapor inside the reactor. The four heating zones of the furnace heater are digitally controlled using separate two-point (heat only) temperature controllers (Horst R2400, Frankfort, Germany) with LCD Display). The temperatures in each of the four zones are adjustable based on the top and the bottom temperature. By maintaining the four temperatures in each zone the entire membrane reactor is operated at a desired reaction temperature.

## EXPERIMENTAL PROCEDURE

Two membrane sizes were used for the evaluation (10mm OD and 25 mm OD respectively) with a length of 368 mm in each case. Tests were performed at atmospheric pressure, 800 °C and 900 °C and at four different volumetric flowrates (517, 994, 1,656 and 3,312 ml/min). Before the reaction, the entire flow system was flushed with N<sub>2</sub> for about 15 to 20 minutes at a flow rate of 100 mL/min at room temperature. Subsequently, it was heated up to the desired reaction temperature. Once the desired temperature had been attained, the N<sub>2</sub> flow was switched off and the reactant feed gases were introduced to initiate the reaction. A condenser placed at the reactor outlet collected any water produced during the experiments. The gaseous products were analyzed using an Agilent Technologies Model 7890B equipped with an Agilent Technologies 5977A MS detector and a Varian CP – 3800 gas chromatograph equipped flame ionization detector (FID) and thermal conductivity detector (TCD) respectively. With the recovered water and the product gaseous stream compositions, the CH<sub>4</sub>, O<sub>2</sub> and CO<sub>2</sub> conversions and the H<sub>2</sub>/CO ratios were calculated using an iterative method and closing the mass balances to within a error margin of ± 3%.

## RESULTS AND DISCUSSION

The conversion rates of different types of catalysts on a 15nm g-alumina support (NO<sub>2</sub>) and 6000nm g-alumina support (SO<sub>2</sub>) at 800°C and the flow rate of 0.45Lmin<sup>-1</sup> were tested. We selected the Al<sub>2</sub>O<sub>3</sub>/MgO/Rh 6,000nm membrane to study the effect of exposure to NO<sub>2</sub> contaminant on catalyst performance due to the superior performance of this system compared to the other systems studied. O<sub>2</sub> exhibited the highest conversion (99%) for g-alumina/Rh membrane in contrast to CH<sub>4</sub> and CO<sub>2</sub>. Also, it was found that CH<sub>4</sub> and O<sub>2</sub> exhibited 99.9% conversion for the g-alumina/MgO/Rh membrane in contrast to CO<sub>2</sub> before the NO<sub>2</sub> and SO<sub>2</sub> contaminant tests with the membrane.

### Effect of NO<sub>2</sub> Contaminant on the CO<sub>2</sub>, CH<sub>4</sub> and O<sub>2</sub> Conversions

Figure 4 shows the conversion rates of different types of catalysts on a 15nm g-alumina support (NO<sub>2</sub>) and 6000nm g-alumina support (SO<sub>2</sub>) at 800°C and the flow rate of 0.45Lmin<sup>-1</sup>. We selected the Al<sub>2</sub>O<sub>3</sub>/MgO/Rh 6,000nm membrane to study the effect of exposure to NO<sub>2</sub> contaminant on catalyst performance due to the superior performance of this system compared to the other systems studied. From figure 11, it can be seen that the O<sub>2</sub> exhibited the highest conversion (99%) for g-alumina/Rh membrane in contrast to CH<sub>4</sub> and CO<sub>2</sub>. Also, it was found that CH<sub>4</sub> and O<sub>2</sub> exhibited 99.9% conversion for the g-alumina/MgO/Rh membrane in contrast to CO<sub>2</sub> before the NO<sub>2</sub> and SO<sub>2</sub> contaminant tests with the membrane.

### Time-Dependent Stability Conversions of CO<sub>2</sub>, CH<sub>4</sub> and O<sub>2</sub> in SO<sub>2</sub> and NO<sub>2</sub> Contaminants

Figure 5 shows the time-dependent activities (stability) of the membranes for NO<sub>2</sub> (a) and SO<sub>2</sub> contaminants (b) on Rh catalysts. On the 15 nm pore size g-Al<sub>2</sub>O<sub>3</sub>/MgO/Rh (NO<sub>2</sub> contaminant), the conversions of CH<sub>4</sub> and O<sub>2</sub> remained virtually unchanged during the seven-hour testing period of study. CO<sub>2</sub> also showed a

stable conversion during the period of study and its conversion improved steadily. Initially, the CO<sub>2</sub> conversions were slightly lower than those observed for CH<sub>4</sub> and O<sub>2</sub> but increased noticeably after the first 2 hours, and again after the first 5 hours to become almost unchanged from 6 to 7 hours. No significant deactivation occurred. We selected the Al<sub>2</sub>O<sub>3</sub>/MgO/Rh 15nm membrane to study the effect of exposure to NO<sub>2</sub> contaminant and the 6000 nm pore size to study the effect of exposure to SO<sub>2</sub> contaminant on catalyst performance due the superior performance of Al<sub>2</sub>O<sub>3</sub>/MgO system compared to the other systems studied tested.

### **Effect of Inlet Carbon Dioxide Concentration in the Feed on Syngas Quality**

Figure 6 shows the effect of carbon dioxide concentration on the quality of syngas produced. Carbon dioxide re-forming is typically influenced by the simultaneous occurrence of the reverse water gas shift (RWGS) reaction (equation 8), which results in H<sub>2</sub>/CO ratios of less than 2. In traditional fixed-bed reactors, this ratio is usually less than unity. Results of flue gas reforming of CH<sub>4</sub> by three catalysts (Ni/Ce – ZrO<sub>2</sub>, Ni/ZrO<sub>2</sub> and Haldor Topsoe R-67-7H) have revealed that the coke on the reactor wall and the surface of catalyst were reduced dramatically. It was found that the weak acidic sites, basic site and redox ability of Ce-ZrO<sub>2</sub> play an important role in methane conversion. This is an important finding. It confirms that the FFCM can be used to carryout reforming of other feedstocks apart from flue gas. Enormous quantities of co-produced gas are flared as a waste by-product during gas processing. In the upgrading of bitumen, the offgas is wasted to the atmosphere instead of being utilised and in landfills the current practice involves the separation of methane and CO<sub>2</sub> with the CO<sub>2</sub> being vented into the atmosphere. The concentration of CO<sub>2</sub> in these applications varies and our results show that the syngas produced by varying the CO<sub>2</sub> concentration in the feed from 5 to 40% has an H<sub>2</sub>: CO ratio varying from 2 – 1.7 respectively. This syngas quality range is within the desired window for the production of several value-added carbon-based products such as hydrogen, methanol, ammonia and gas-to-liquids (GTL).

### **CONCLUSIONS**

To overcome this major drawback of equations 5 and 6 we have developed a flow-through catalytic membrane reactor in which the reactants are forced-through the interconnected pores of the thickness of the membrane which is impregnated with highly-dispersed nano-sized catalysts. The pore size and porosity of the membrane is carefully selected such that there is not significant segregation of the reactants in the membrane due to molecular weight difference but after the chemical reaction occurs, the generated H<sub>2</sub> is transported away from the catalytic surface at a much faster rate away from the reaction zone due to Knudsen flow. This enhances the further conversation of the feed as a result of equilibrium shift and thus increases the conversion. Additionally, this phenomenon also eliminates cocking and the Boudaouard reaction is eliminated. This opens the door for commercialisation of the process.

### **REFERENCES**

- [1] GANESH R. ET AL. (2017) JOURNAL OF CO<sub>2</sub> UTILIZATION, VOLUME 18,PAGES 318-325
- [2] AITOROCHOA ET AL. (2020) RENEWABLE AND SUSTAINABLE ENERGY REVIEWS, VOLUME 119, 109600

### **ACKNOWLEDGEMENTS**

This work was supported by the Emissions Reduction Alberta (Grant # EO1#K130073), Canada

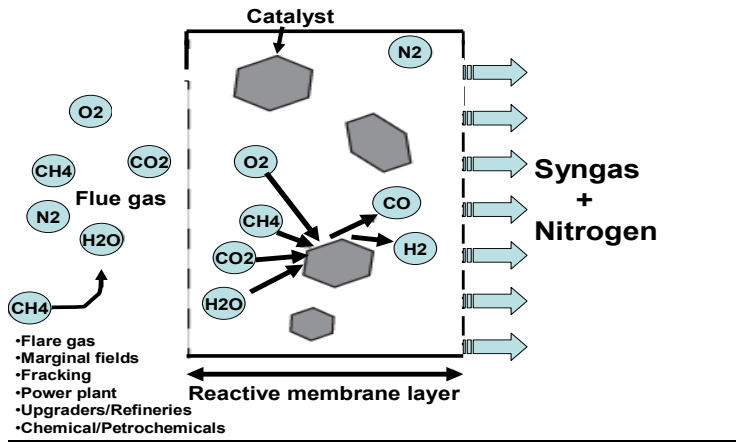


**Figure 1: Schematic Diagram of the membrane operating in the Forced Flow-through configuration**

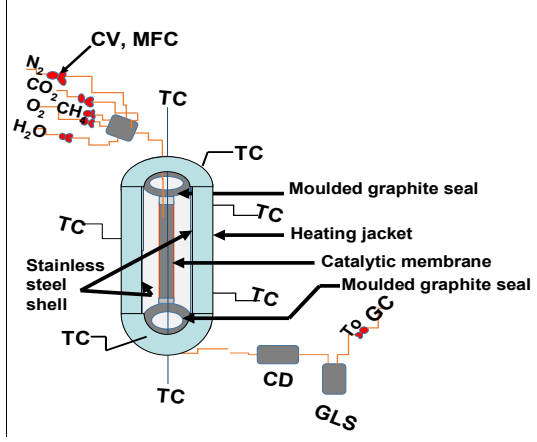


**Figure 2: Schematic Diagram of the Reactor Feed Flow**



**Figure 3: Photograph of the Two Membrane Reactors Enclosed in the Heating Furnace (Heating Jacket) with Power Controllers between the Reactors and Showing the Thermocouples**

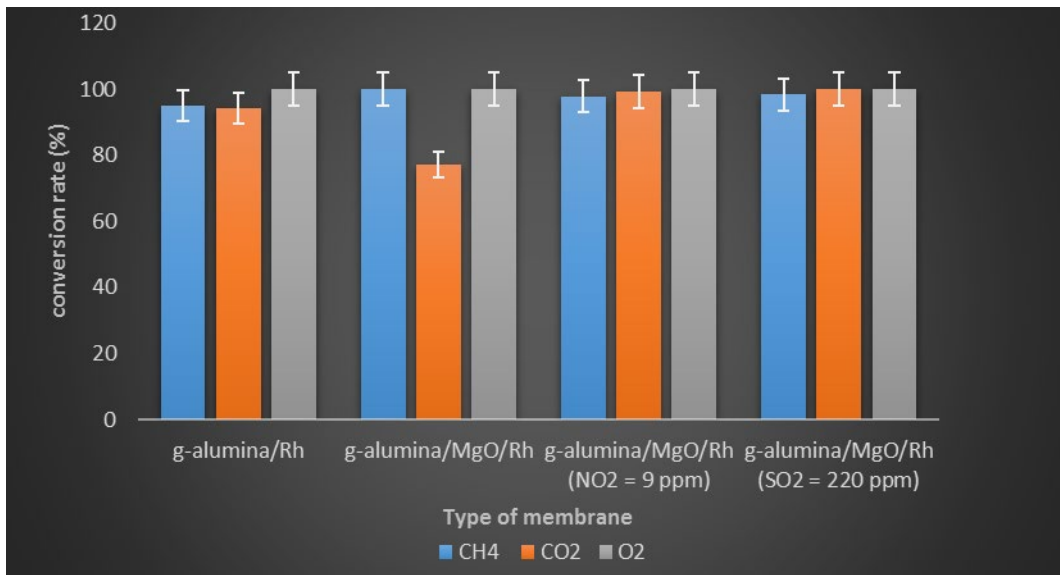


Figure 4: Effect Temperature on O<sub>2</sub>, CO<sub>2</sub> and CH<sub>4</sub> Conversion on g-Al<sub>2</sub>O<sub>3</sub>/Rh, g-Al<sub>2</sub>O<sub>3</sub>/MgO/Rh, and Effect of NO<sub>2</sub> and SO<sub>2</sub> Impurities on O<sub>2</sub>, CO<sub>2</sub> and CH<sub>4</sub> Conversion on g-Al<sub>2</sub>O<sub>3</sub>/MgO/Rh (NO<sub>2</sub>/Al<sub>2</sub>O<sub>3</sub>/MgO/Rh = 15 nm pore size and SO<sub>2</sub>/Al<sub>2</sub>O<sub>3</sub>/MgO/Rh = 6000 nm pore size; Feed flowrate = 0.45L/min; Rh catalyst loading = 0.7 wt % Rh; Temperature = 800 °C).

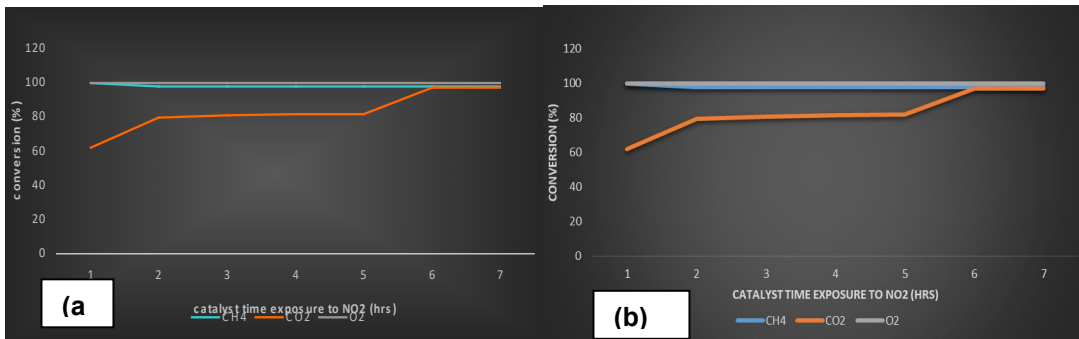


Figure 5: Stability of 15 nm Pore Size g-Al<sub>2</sub>O<sub>3</sub>/MgO/Rh Membrane after Exposure to 9ppm NO<sub>2</sub> at 800 °C (flowrate = 0.37 Lmin<sup>-1</sup>) (a) and Stability of 6000 nm Pore Size g-Al<sub>2</sub>O<sub>3</sub>/MgO/Rh Membrane after Exposure to 220ppm SO<sub>2</sub> at 800 °C (Feed flowrate = 0.37 Lmin<sup>-1</sup>) (b)

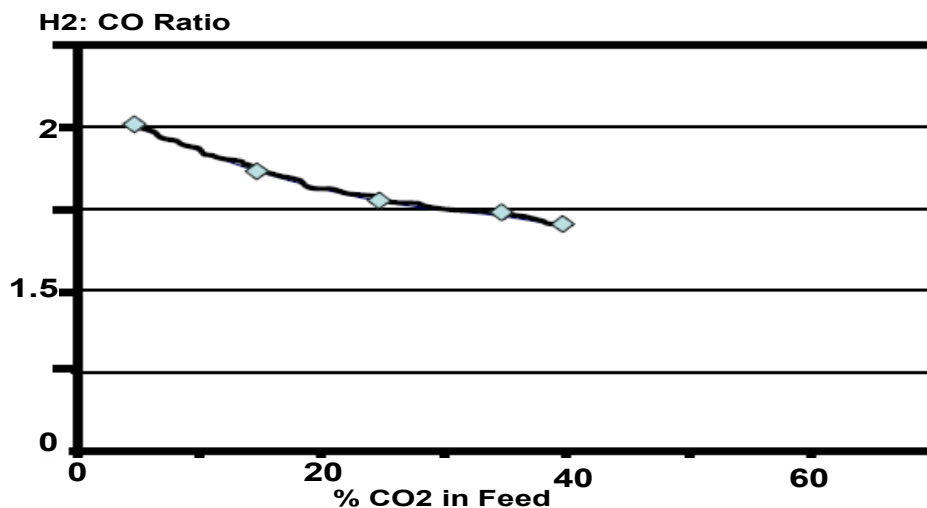


Figure 6: Effect of Feed Carbon Dioxide Concentration on the Syngas Quality